

We are IntechOpen, the world's leading publisher of Open Access books Built by scientists, for scientists

5,300

Open access books available

130,000

International authors and editors

155M

Downloads

Our authors are among the

154

Countries delivered to

TOP 1%

most cited scientists

12.2%

Contributors from top 500 universities



WEB OF SCIENCE™

Selection of our books indexed in the Book Citation Index
in Web of Science™ Core Collection (BKCI)

Interested in publishing with us?
Contact book.department@intechopen.com

Numbers displayed above are based on latest data collected.
For more information visit www.intechopen.com



MNLR and ANFIS Based Inductance Profile Estimation for Switched Reluctance Motor

Susitra Dhanarajalu

Abstract

This chapter aims in presenting the methods for the accurate estimation of highly non linear phase inductance profile of a switched reluctance motor (SRM). The magnetization characteristics of a test SRM is derived from the SRDaS (Switched Reluctance Design and Simulation) simulation software. Statistical interpolation based regression analysis and Artificial Intelligence (AI) techniques are used for developing the computationally efficient inductance model. Multi Variate Non linear Regression (MVNLR) from the class of regression analysis and Adaptive Neuro Fuzzy Inference System (ANFIS) under the class of AI are implemented and tested on the simulated data. Non linear Inductance profile $L(I, \theta)$ of SRM is successfully estimated for the complete working range of phase currents (I_{ph}). At each I_{ph} , $L(I, \theta)$ values are estimated and presented for one cycle of rotor position (θ). Estimated inductance profile based on the two proposed methods is observed to be in excellent correlation with the true value of data.

Keywords: SRM, electromagnetic profile, multivariate non-linear regression, ANFIS

1. Introduction

Over past two decades, there has been noticeable increase in the research publications on switched reluctance machine (SRM). The machine can be operated as both generator and motor by suitable control techniques. It has been proved from research publications that SRM is a valid alternative to conventional machines in almost all industrial applications. The characteristics of electromagnetic parameters are highly non-linear due to the following reasons; i) highly saturated working zone ii) eddy current and hysteresis current effects iii) double salient structure and iv) non uniform air gap. All these effects makes the machine's flux linkage and torque as the non-linear function of phase current (I_{ph}) and rotor position (θ). Flux linkage of the machine depends on its phase inductance. For the analysis and control of the machine, it is important to establish the accurate nonlinear mapping between its phase inductance, phase current and rotor position. The design and electrical analysis of the machine is greatly dependent on its electromagnetic behavior. Linear mathematical models are proposed by many publications that are not applicable for real time control. Non-linear models are developed by few researchers based on the following techniques; a) Analytical model [1–10] in which Fourier series based

expressions are derived. This method is highly time consuming and not suitable for real time control applications. b) magnetic model [11] c) finite element model (FEM) [11, 12] provides accurate results whereas it involves complicated mathematics computation. d) Artificial neural network models [13–21].

All these models have either fine precision or good computation speed. Both the benefits are not satisfied in any of these models. Few of the recent research publications have reported using the Adaptive Neuro fuzzy inference system (ANFIS) techniques for the computation of magnetic parameters [22–24] and estimation of rotor position [25]. On the overview of the publications on modeling of SRM, it is observed that none of the papers have paid attention in using Multivariate nonlinear regression technique (MVNLRT) for estimating its nonlinear inductance model. In this chapter, non-linear inductance model of SRM is developed based on the MVNLRT and ANFIS. Also the comparison between the results of ANFIS and MVNLRT inductance models are presented. This chapter is organized as follows; Section II discusses the mathematical model of SRM and the necessity of inductance modeling. The nonlinear inductance model based on MVNLRT and the one based on ANFIS are presented in section III and IV respectively. The comparative analysis of both the models is presented in section V and the inferential remarks are given in section VI.

2. Mathematical model of SRG and the necessity of inductance modeling

SRM is a singly excited and doubly salient machine shown in **Figure 1**. The number of phases wound on the stator poles differs from machine to machine. There is certain number of suitable combinations of stator and rotor poles thus giving many machine configurations. The phase windings are excited sequentially for rotating the rotor in desired direction. For efficient control, the phase windings are excited with the current pulses based on the rotor position.

The electromagnetic characteristics of the machine vary depending on the relative rotor position with respect to stator pole axis and magnitude of current in the excited phase winding. An ideal machine is one with equal stator and rotor pole axis and saturation of the core and leakage fluxes are neglected. In such a ideal machine,

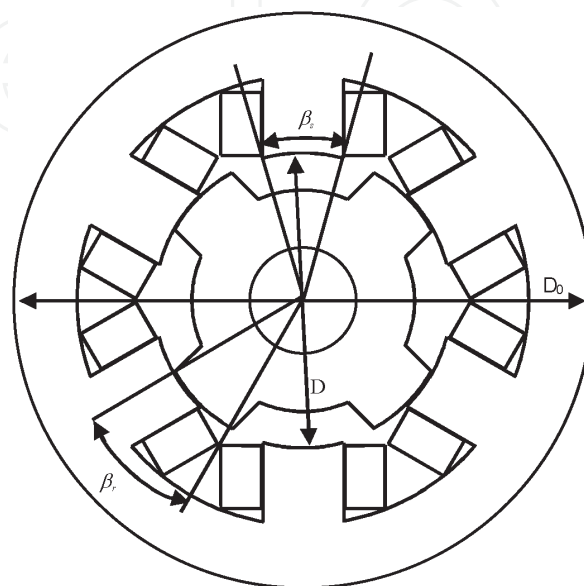


Figure 1.
Three phase 6/4 pole SRM configuration.

the variation of phase inductance is triangular in shape. However, in a practical machine, the variation is highly nonlinear. When the stator and rotor poles are coincident (aligned position), the inductance is maximum and minimum inductance is experienced when the rotor inter polar axis coincides with the excited stator pole axis (unaligned position). The position of rotor between these two positions is called intermediate positions. Upon exciting a particular stator phase, its nearest pair of rotor poles tends to move towards the path of minimum reluctance along the excited stator poles by developing a required torque. The magnitude of torque developed depends on the magnitude of the excited current and rate of change of inductance with rotor position. Accurate rotor position sensors, power converter and a controller with good control technique are required for the successful operation and precise control of SRM [26].

Owing to the high non-linearity of the machine, a mathematical model describing the behavior of the machine is required. This model can be used as a base for simulation and verification of static and dynamic characteristics of SRM.

2.1 Energy balance equation

The conversion of electrical energy to mechanical energy and vice versa by an electromechanical energy converter is illustrated by the energy-balance scheme shown in **Figure 2**.

A magnetic system couples the electrical and mechanical systems. The electro-mechanical energy converter illustrates the relationship between the electrical energy, mechanical energy, energy losses, energy stored and energies transferred between the electrical and mechanical systems. From **Figure 2**, and making an assumption that $W_{iron} = 0$ and $W_{leak} = 0$, the following equations are developed.

$$W_{ea} = W_{ei} - W_{cu} - W_{leak} \quad (1)$$

$$W_{emec} = W_{ea} - W_{field} - W_{iron} \quad (2)$$

$$W_{mech} = W_{emec} - W_{fri} - W_{iner} \quad (3)$$

$$\text{Energy input} = W_{ea} \quad (4)$$

$$\text{Energy losses} = W_{cu} + W_{iron} + W_{fri} \quad (5)$$

$$\text{Energy stored in the system} = W_{leak} + W_{field} + W_{iner} \quad (6)$$

$$\text{Energy output} = W_{mech} \quad (7)$$

Thus Energy output = Energy input - Energy losses - Energy stored.

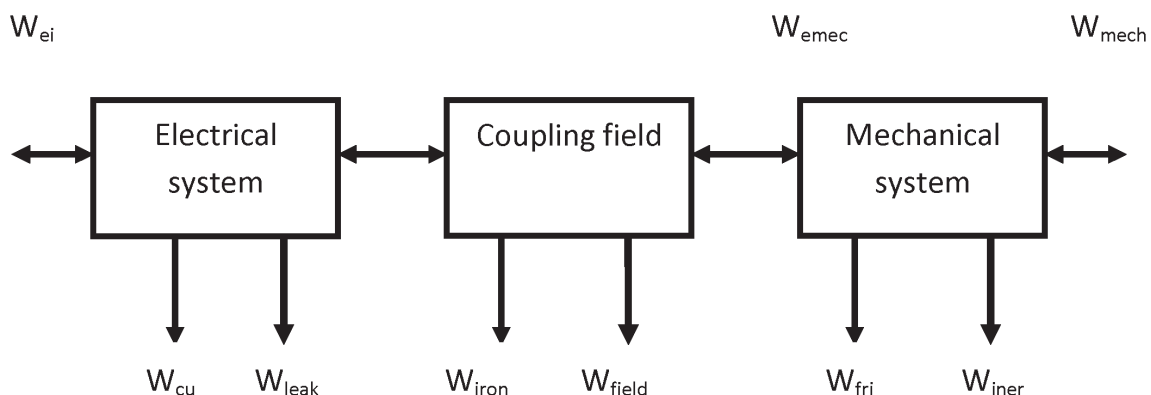


Figure 2.
 Electromechanical energy conversion model.

In an ideal system, if the energy losses are neglected, the output energy is equal to the energy input into the system minus energy stored in the various components of the system. However, the stored energies can be recovered through regenerative process.

2.2 Equation of phase voltage

Electromagnetic characteristics of a 6/4 pole SRM is shown in **Figure 3**. The illustration shows the mapping among the flux linkage (ψ), current (i) in excited phase and rotor position (θ) of SRM. The high non-linearity behavior of the machine is clearly visible from the figure. The curve is linear for small values of excitation current. As the rotor rotates from unaligned to aligned position, the mapping among the motor parameters becomes highly nonlinear.

Figure 4 shows the equivalent circuit of an excited phase of the motor.

According to **Figure 4**, the instantaneous voltage across the terminals of a phase of SRM winding related to the flux linked in the winding is given by,

$$V_{ph}(t) = i_{ph}(t)r_{ph} + \frac{d\psi_{ph}(i_{ph}, \theta_{ph})}{dt} \quad (8)$$

$$\psi_{ph} = \int (V_{ph} - i_{ph}r_{ph})dt \quad (9)$$

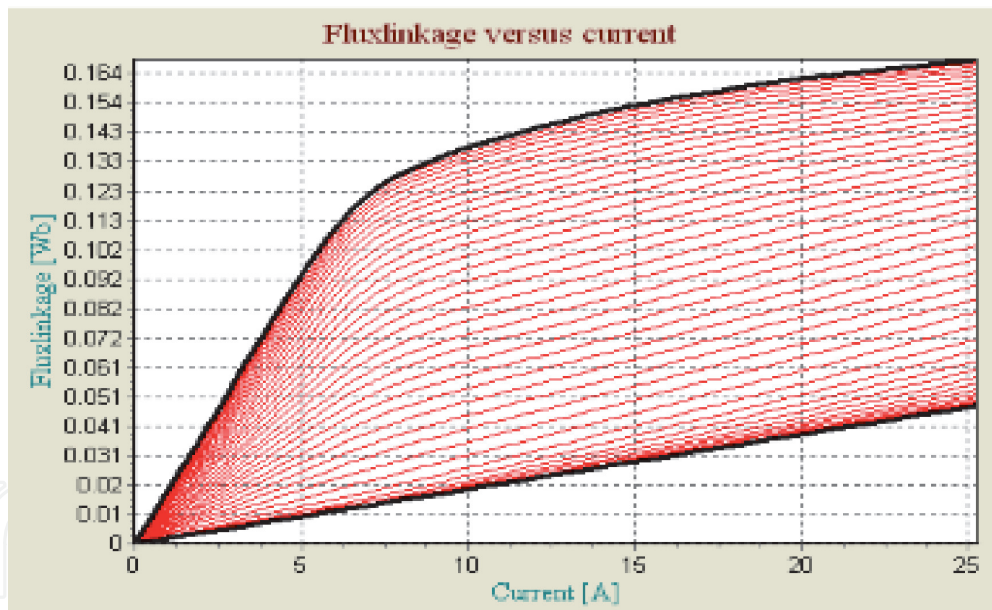


Figure 3.
Magnetization characteristics of three phase 6/4 pole SRM.

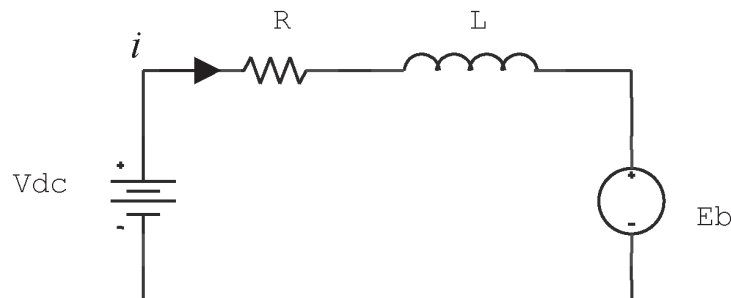


Figure 4.
Electrical equivalent circuit of the SRM.

Due to the double salient structure and effect of magnetic saturation, the flux linkage (ψ_{ph}) and inductance of excited motor phase winding varies as a function of both rotor position (θ_{ph}) and phase current (i_{ph}). Therefore (8) is written as given in (10).

$$V_{ph} = i_{ph}r_{ph} + \frac{d[L_{ph}(i_{ph},\theta), i_{ph}]}{dt} \quad (10)$$

$$V_{ph} = i_{ph}r_{ph} + L_{ph} \frac{di_{ph}}{dt} + i_{ph} \frac{\partial L_{ph}}{\partial \theta} \frac{d\theta}{dt} \quad (11)$$

$$V_{ph} = i_{ph}r_{ph} + \left[L_{ph} \frac{di_{ph}}{dt} + \frac{1}{2} i_{ph} \frac{dL_{ph}}{d\theta} \omega \right] + \frac{1}{2} i_{ph} \omega \frac{dL_{ph}}{d\theta} \quad (12)$$

2.3 Torque equation

When a phase of the SRM is excited by a voltage source, the instantaneous power is obtained by multiplying (12) by i_{ph} .

$$P = V_{ph}i_{ph} = i_{ph}^2 r_{ph} + i_{ph} L_{ph} \frac{di_{ph}}{dt} + \omega i_{ph}^2 \frac{dL_{ph}}{d\theta} \quad (13)$$

$$V_{ph}i_{ph} = i_{ph}^2 r_{ph} + \frac{d}{dt} \left(\frac{1}{2} L_{ph} i_{ph}^2 \right) + \frac{1}{2} \omega i_{ph}^2 \frac{dL_{ph}}{d\theta} \quad (14)$$

$$V_{ph}i_{ph} = i_{ph}^2 r_{ph} + \frac{dw_f}{dt} + T_m \omega \quad (15)$$

where

$$W_f = \frac{1}{2} L_{ph} i_{ph}^2 \quad (16)$$

is the energy stored in the magnetic field.
and

$$T_m = \frac{1}{2} i_{ph}^2 \frac{dL_{ph}}{d\theta} \quad (17)$$

is the expression for instantaneous torque produced in the energized phase winding. In (15), The instantaneous electrical power supplied to the motor is given on the left hand side of the equation. On the right hand side of equation, the first term represents the power loss due to phase resistance, the derivative of stored energy in the magnetic field is represented in the second term and the mechanical power developed by the motor is represented in the third term.

The stator and rotor pole arc combinations are equal in SRM. The machine has triangular shaped inductance characteristics. The inductance value is maximum at aligned position and minimum at unaligned position. For a 6/4 pole SRM, an inductance profile for unequal stator and rotor pole arc combinations are shown in **Figure 5**. From the Eq. (17), it is clear that SRM develops positive torque when the phase is excited during the period of rising inductance, when $\frac{dL}{d\theta} > 0$. Negative torque is developed when the phase is excited during the period of the falling inductance, when $\frac{dL}{d\theta} < 0$ and torque developed is zero when the phase is excited during the period of constant inductance, when $\frac{dL}{d\theta} = 0$. The machine can transform reversible modes of motoring and generating operations by suitable control of the switches in power converter. From this, it is understood that the operating mode of

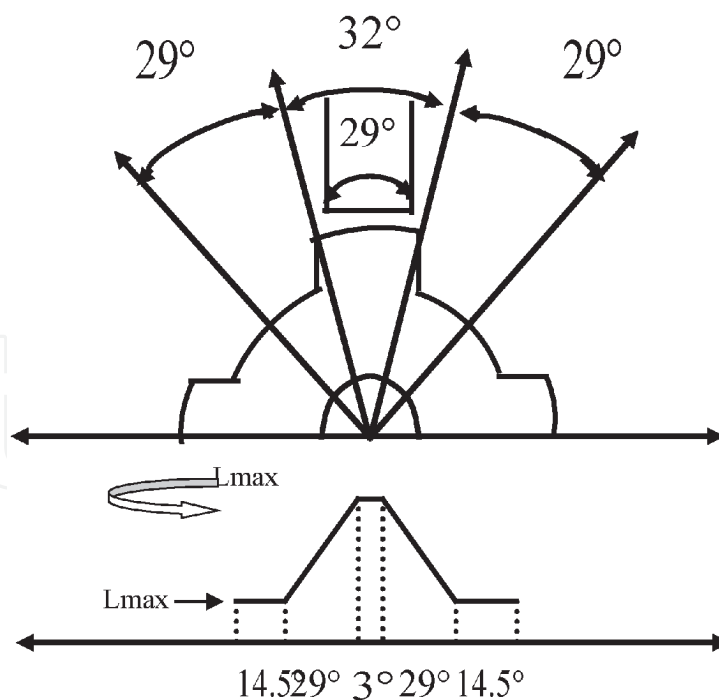


Figure 5.
Variation of inductance for one rotor pole pitch.

the machine greatly depends on its phase inductance value. Therefore inductance needs to be modeled accurately for real time applications.

The torque developed can be normally expressed in terms of the change of coenergy with respect to rotor position. The $\Psi - i$ characteristics of the SRM for a given rotor position is shown in **Figure 6**. These characteristics can either be obtained by conducting an experiment on the SRM or by performing magnetic field analysis. The area representing stored field energy (W_f) and co-energy (W_c) are marked in **Figure 6(a)** for a given phase current. The area below the $\psi - i$, characteristics can be written as.

$$W_c = \int_0^i \psi di \quad (18)$$

Consider the movement of the rotor through an infinitesimal displacement $\Delta\theta$ when the current is held constant. The $\psi - i$ characteristics of SRM for the given rotor position is shown in **Figure 6(b)**. During the movement of the rotor, a definite amount of mechanical work is done by the motor. The electrical energy (ΔW_e) fed to the motor is partially used to produce mechanical motion (ΔW_m) and a part of the energy gets stored in the magnetic field (ΔW_f). From **Figure 6(b)**, the change in electrical energy input is,

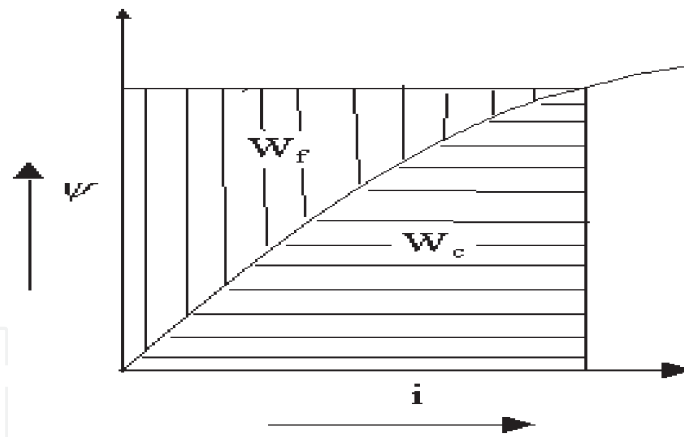
$$\Delta W_e = \text{area WXYZ} \quad (19)$$

and the change in stored field energy is

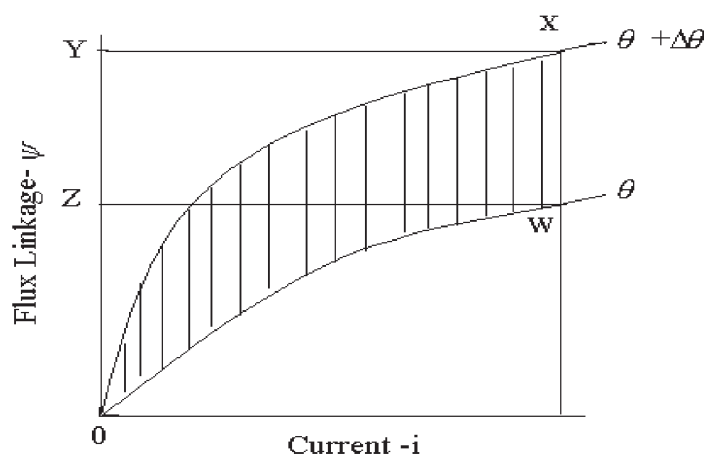
$$\Delta W_f = \text{area OXY} - \text{area OWZ} \quad (20)$$

and the mechanical work done is,

$$\begin{aligned} \Delta W_m &= \Delta W_e - \Delta W_f = T\Delta\theta = \text{Area WXYZ} - (\text{area OXY} - \text{area OWZ}) \\ &= \text{Area WXYZ} - \text{area OXY} - \text{area OWZ} = \text{Area OWX} \end{aligned} \quad (21)$$



(a)



(b)

Figure 6. Magnetic characteristics of SRM. (a) Electromechanical energy conversion. (b) $\psi - i$ characteristics for a given rotor position.

The area OWX represents the change in the co-energy (ΔW_c) and the torque can be calculated as.

$$T = \frac{\Delta W_c}{\Delta \theta} \quad (22)$$

It can be observed that only a part of the energy input into the motor is utilized for torque production. If the $\psi - i$ characteristics were highly non-linear in the aligned position and linear in the unaligned position, then, the magnitude of the torque developed would be higher compared with the situation when the $\psi - i$ characteristics are linear for both the positions.

3. Inductance modeling of SRM using multivariate nonlinear regression technique

Regression analysis uses many techniques for modeling and analyzing parameters. It is useful in accurate mapping of dependent and independent variables even under unknown physical process. In non-linear regression model, the observed data

are expressed as a nonlinear function of parameters and proved to be more accurate even for extrapolated data range. A nonlinear model is expressed as given in (23).

$$y = f(X, \beta) + \varepsilon \quad (23)$$

where

- y - Vector of the observed response variables ($n \times 1$).
- X - matrix determined by the predictor variables ($n \times p$).
- β - vector of unknown parameters to be estimated ($p \times 1$).
- f - function of X and β .
- ε - vector of independent, identically distributed random disturbances ($n \times 1$).

Multivariate analysis encompasses the observation and analysis of more than one outcome variable and gives an excellent solution for nonlinear problems. This approach executes well in high dimensional problems especially when the available data set is of very small size. In this section MVNLR model is used for estimating the inductance parameters. Coefficients of predictor variables are estimated using least square method. The inductance values between an unaligned and aligned position from the magnetization characteristics of [27] has been used in exploring the non-linear relationships between the phase inductance $L(i, \theta)$, phase current (I) and rotor position (θ) and is expressed in terms of least square polynomial approximation of third order and the MVNLR based inductance model of the three phase, 6/4 SRG is expressed by the Eq. (24).

$$\begin{aligned} \begin{bmatrix} L_1 \\ L_2 \\ L_3 \end{bmatrix} &= \begin{bmatrix} 2.605 \times 10^{-6} & -9.645 \times 10^{-5} & 9.933 \times 10^{-4} \\ 2.631 \times 10^{-6} & -9.741 \times 10^{-5} & 10.032 \times 10^{-4} \\ 2.579 \times 10^{-6} & -9.549 \times 10^{-5} & 9.834 \times 10^{-4} \end{bmatrix} \begin{bmatrix} I^3 \\ I^2 \\ I \end{bmatrix} + \\ &\begin{bmatrix} -5.518 \times 10^{-8} & 1.914 \times 10^{-7} & 3.752 \times 10^{-4} \\ -5.573 \times 10^{-8} & 1.933 \times 10^{-7} & 3.79 \times 10^{-4} \\ -5.463 \times 10^{-8} & 1.894 \times 10^{-7} & 3.714 \times 10^{-4} \end{bmatrix} \begin{bmatrix} \theta^3 \\ \theta^2 \\ \theta \end{bmatrix} + \\ &\begin{bmatrix} -5.825 \times 10^{-7} & 1.881 \times 10^{-7} & -2.745 \times 10^{-6} \\ -5.883 \times 10^{-7} & 1.91 \times 10^{-7} & -2.772 \times 10^{-6} \\ -5.767 \times 10^{-7} & 1.862 \times 10^{-7} & -2.718 \times 10^{-6} \end{bmatrix} \begin{bmatrix} I^2 \theta \\ I \theta^2 \\ I \theta \end{bmatrix} + \\ &\begin{bmatrix} -1.095 \times 10^{-3} \\ -1.106 \times 10^{-3} \\ -1.084 \times 10^{-3} \end{bmatrix} \end{aligned} \quad (24)$$

Actual inductance Vs MVNLR inductance

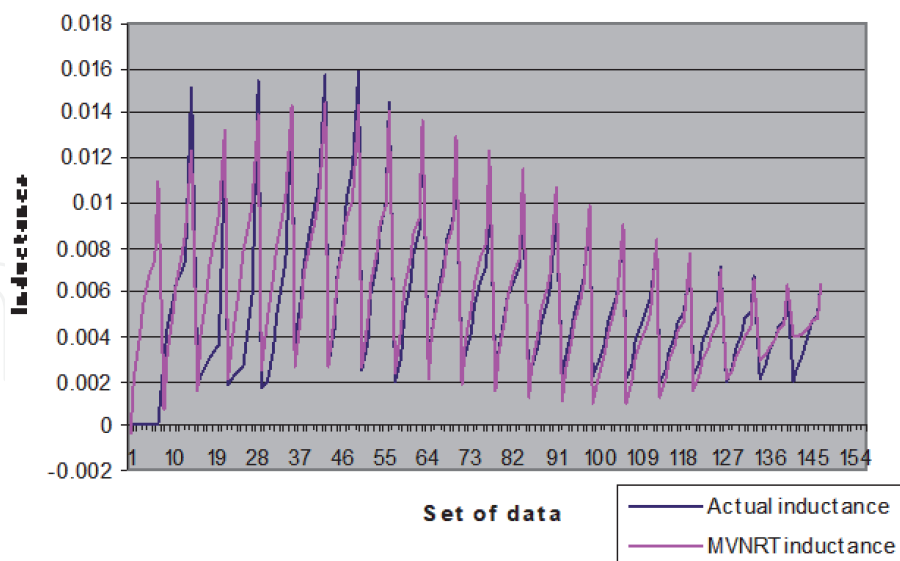


Figure 7.
 True data set vs MVNLR predicted data.

Comparison of true values Vs MVNLR estimated values is shown in **Figure 7**. From the analysis, it is clearly evident that the MVNLR predicted inductance values shows a strong agreement with the true data values used for developing the model.

4. Inductance modeling of SRG using adaptive neuro -fuzzy inference system

The ANFIS is an adaptive neuro - fuzzy inference system (Jyh-Shing et al., 1993) [28]. The fuzzy inference system (FIS) has been developed for the inductance estimation of SR machine. FIS has two inputs and single output. Phase current (I_{ph}) and rotor position (θ) are the input variables and phase inductance, $L(I,\theta)$ is the output variable. The input variables are fuzzified using 12 triangular membership functions. Fuzzy rule base has 12*12 (144) if-then rules. The ANFIS architecture is shown in **Figure 8**. There are 5 layers in the ANFIS network.

Layer 1: Both the inputs are fuzzified with 12 triangular membership functions. The output of input membership function 1 is $O_{k1} = \mu A_k(i)$ and the output of input membership function 2 is, $O_{k2} = \mu B_k(\theta)$, i and θ are the input to nodes 1 and 2, respectively. A_k and B_k are the linguistic labels (mf1, mf2... mf12.) associated with the node functions.

The output of the input membership functions specifies the degree to which the given i and θ satisfies the quantifier A_k and B_k . Triangular shaped membership functions $\mu A_k(i)$ and $\mu B_k(\theta)$ are used with a maximum equal to 1 and a minimum equal to 0. The generalized triangular membership function of the current is given by

$$\mu A_k(i) = \begin{cases} 0 & i \leq a_k \\ \frac{i - a_k}{b_k - a_k} & a_k \leq i \leq b_k \\ \frac{c_k - i}{c_k - b_k} & b_k \leq i \leq c_k \\ 0 & c_k \leq i \end{cases} \quad (25)$$

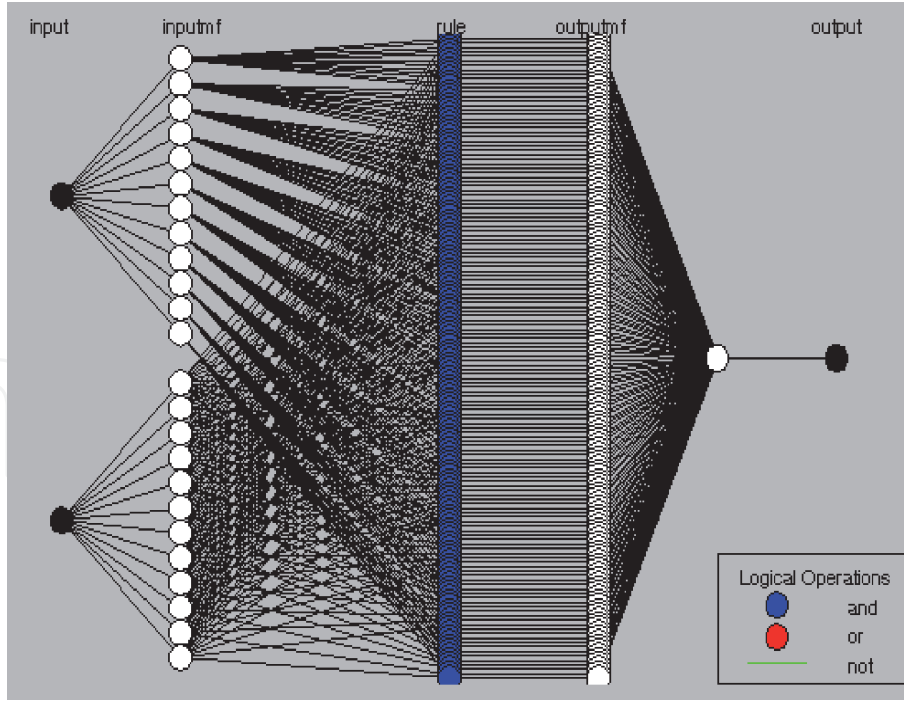


Figure 8.
ANFIS network structure.

Similarly, the generalized triangular shaped membership function of the rotor position is given by

$$\mu B_k(\theta) = \begin{cases} 0 & \theta \leq a_k \\ \frac{\theta - a_k}{b_k - a_k} & a_k \leq \theta \leq b_k \\ \frac{c_k - \theta}{c_k - b_k} & b_k \leq \theta \leq c_k \\ 0 & c_k \leq \theta \end{cases} \quad (26)$$

where a_k , b_k and c_k are the adaptable variables. The triangular shaped functions varies with the change in the parameter values.

Layer 2: Fuzzy AND operator is implemented in this layer.

$$W_k = \mu A_k(i) \times \mu B_k(\theta) \quad (27)$$

where $k = 1, 2 \dots 12$;

Layer 3: Scaling or normalizing of firing strengths takes place in this layer.

$$\bar{W}_k = O_{k4} = \bar{W}_k f_k = \bar{W}_k (m_k + n_k \theta + r_k) \quad (28)$$

Layer 4: The output of the fourth layer comprises a linear combination of the inputs multiplied by the normalized firing strength. Output of this layer is given by.

$$O_{k4} = \bar{W}_k f_k = \bar{W}_k (m_k i + n_k \theta + r_k) \quad (29)$$

Output of layer 3 is \bar{W}_k . The modifiable variables m_k , n_k and r_k are known as consequent parameters.

Layer 5: This layer is a simple summation of the outputs in the previous layer. The phase inductance $L(i,\theta)$ is obtained from the overall output.

$$O_{k5} = \sum \overline{W}_k f_k = \frac{\sum_k W_k f_k}{\sum_k W_k} \quad (30)$$

The magnetic parameter values are considered during the period of unaligned to aligned rotor position for developing the inductance model. The range of the current and rotor position during this period are $0 \leq I \leq 25$ A and $0 \leq \theta \leq 45$ deg.

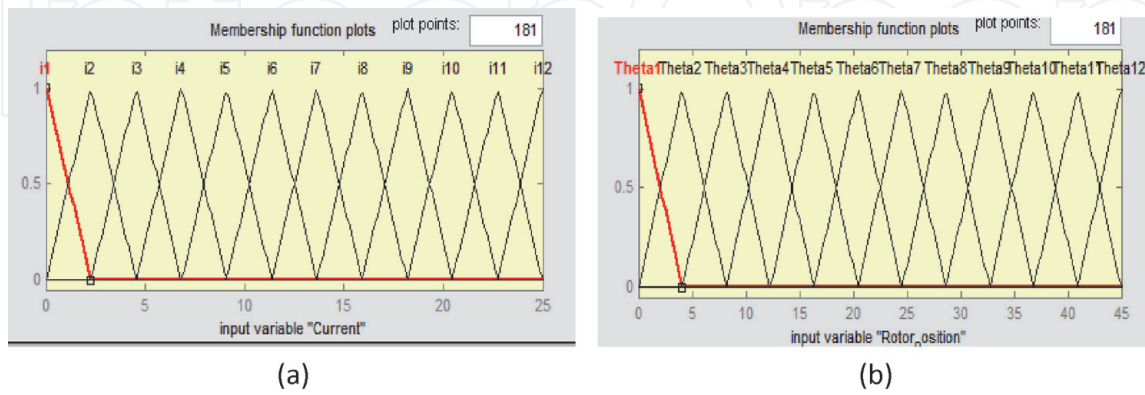


Figure 9. Fuzzy triangular membership functions for the input parameters. (a) Phase current. (b) Rotor position.

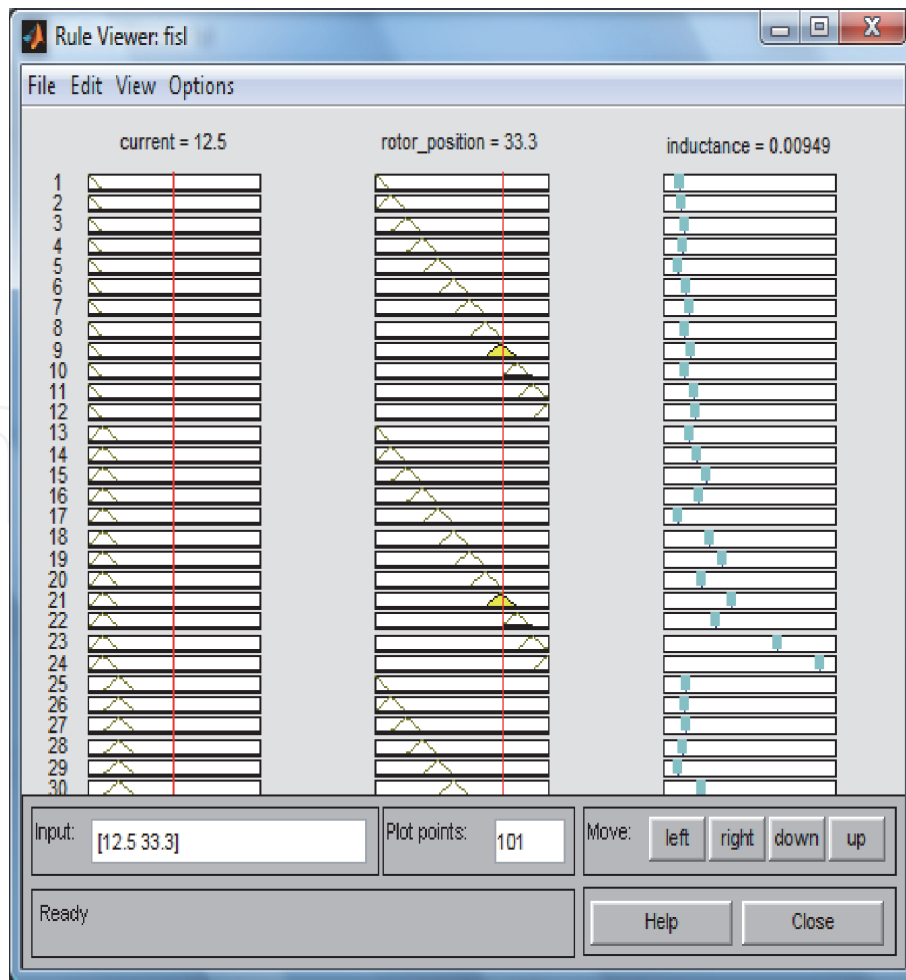


Figure 10. Rule viewer - ANFIS.

The ANFIS information are as follows.

Total number of parameters: 504; Number of nonlinear parameters: 72

Number of linear parameters: 432; Number of fuzzy rules: 144

Number of training data pairs: 182; Number of checking data pairs: 0

Number of nodes: 341.

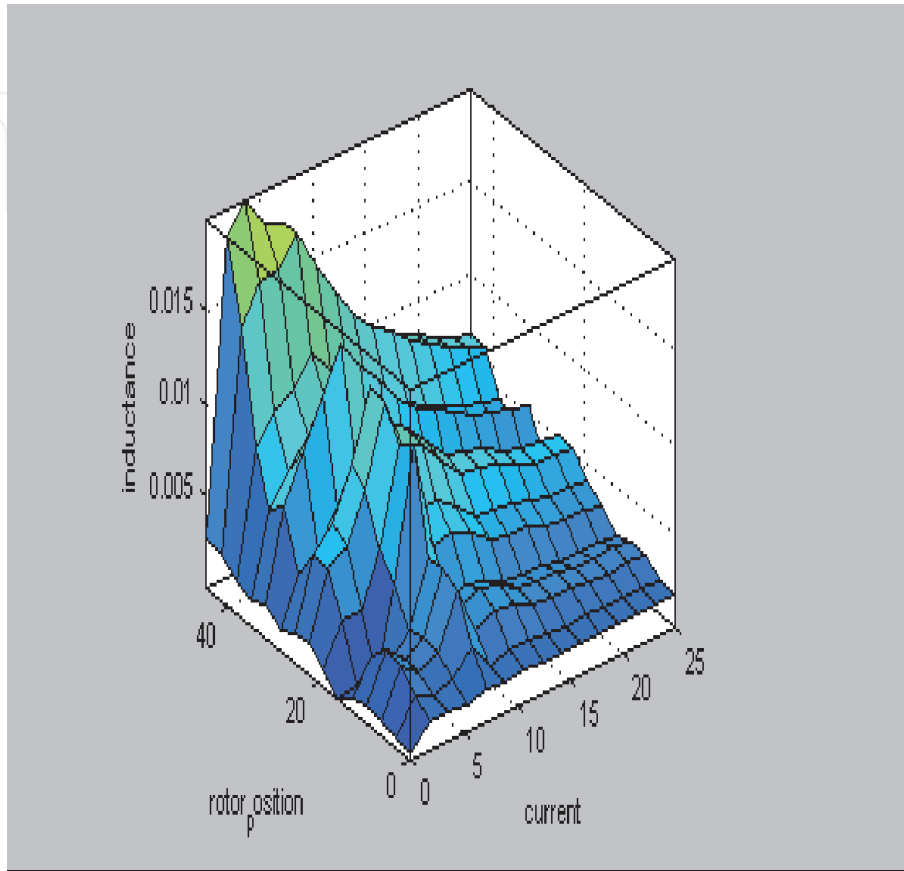


Figure 11.
Mapping surface of $L(i, \theta)$.

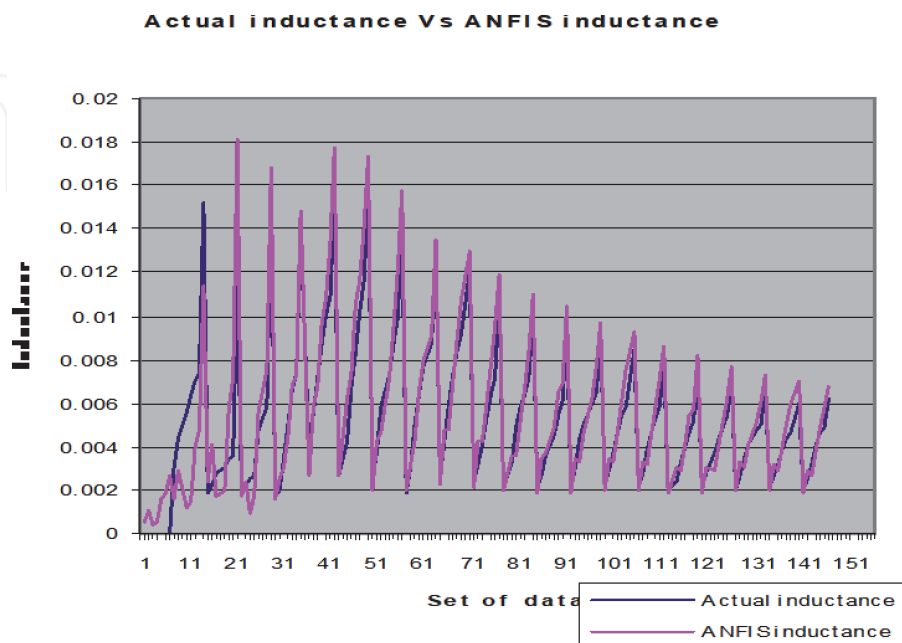


Figure 12.
True data vs ANFIS predicted data.

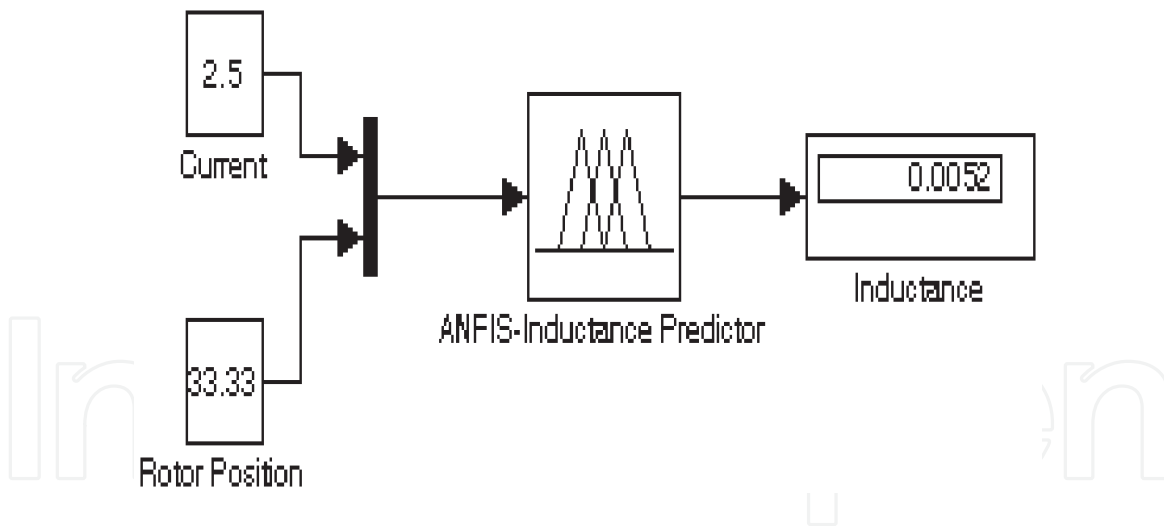


Figure 13.
 ANFIS inductance predictor from Simulink.

The triangular membership functions for the two inputs: current and rotor position are given in **Figure 9(a)** and **(b)** respectively.

The 144 rules framed in ANFIS is shown in **Figure 10**. The fuzzy inference process is interpreted from this rule viewer. The AFIS surface mapping between input and output parameters is depicted in **Figure 11**. For low values of current, the variation in inductance is observed to be linear. After saturation, the variation is highly non linear. **Figure 12** shows the comparison of the original test data with the ANFIS predicted data. From this comparison, it is clear that the inductance estimation from ANFIS is in very good concurrence with the test values of inductance. **Figure 13** shows the MATLAB simulink model of ANFIS inductance predictor.

5. Comparison of MVNLRT and ANFIS based inductance models

Both the proposed inductance models based on MVNLRT and ANFIS uses the data from the magnetization characteristics of the machine. **Figure 14** shows the

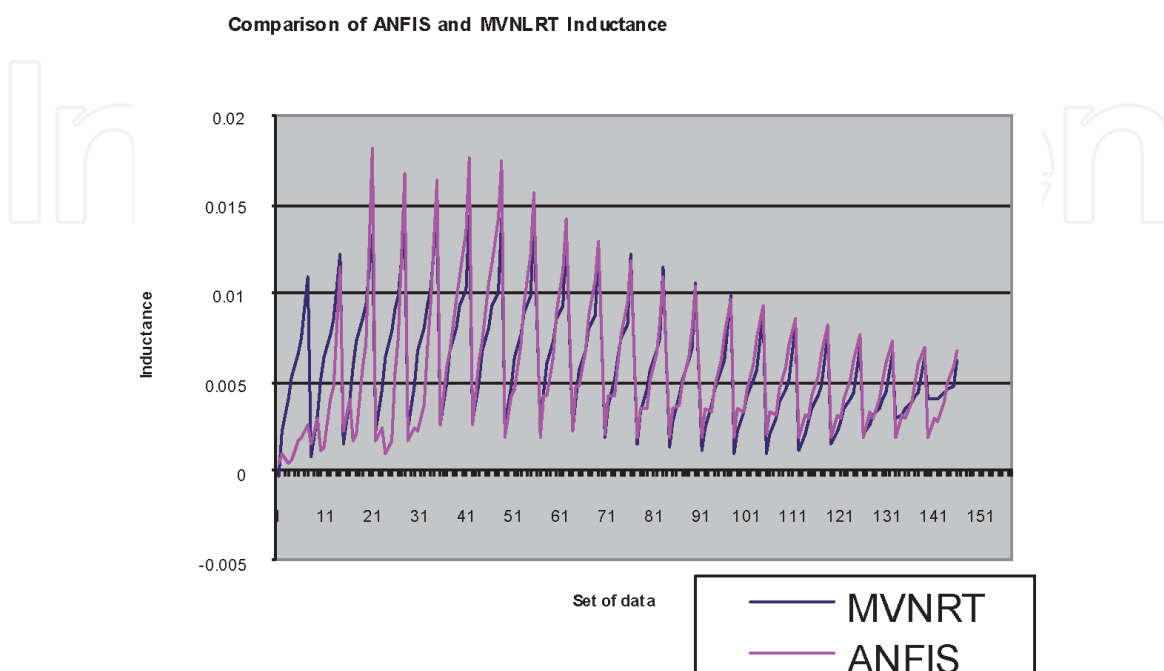


Figure 14.
 MVNLR vs ANFIS models.

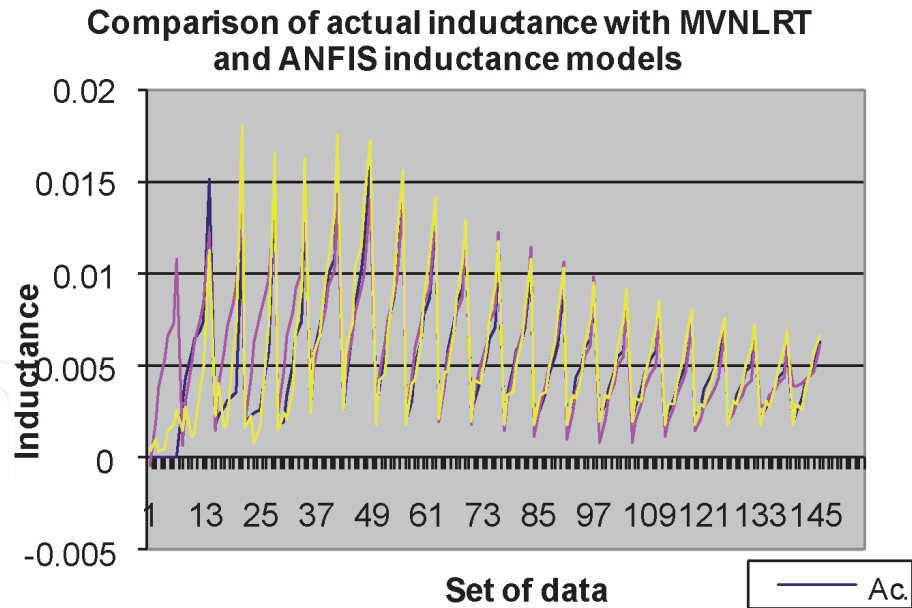


Figure 15. True vs MVNLR vs ANFIS data.

comparison chart of the inductance values obtained from the ANFIS and MVNLRT models and **Figure 15** illustrates the comparison of these two models along with the actual inductance values. For both the methods, the predicted and true values are compared at various phase current values and the same is shown in **Figure 16**. Root-mean-squared error (RMSE), Mean Absolute Error (MAE) and Maximum Absolute value Error (MAVE) for both the methods at different currents are given in **Table 1**. The RMSE for ANFIS and MVNLRT for full range of currents is shown in **Figure 17**. From the careful observation of comparison charts and error values, it is inferred

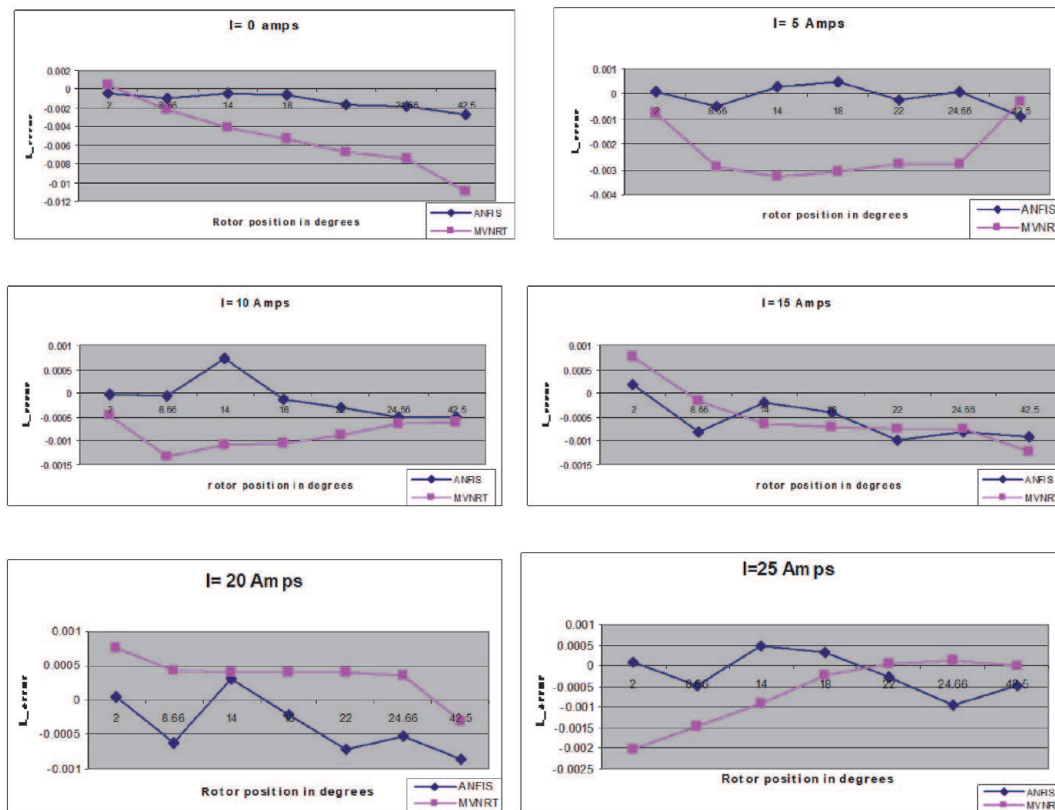


Figure 16. MVNLR VS ANFIS at various currents.

Current in amps	For θ varying from 0 to 45 degrees at each phase current					
	ANFIS Estimator(Error in Henry)			MVNRT Estimator(Error in Henry)		
	$L_{abs\ max}$	$L_{abs\ mean}$	L_{RMSE}	$L_{abs\ max}$	$L_{abs\ mean}$	L_{RMSE}
0	2.7E-03	3E-04	8E-04	1.1E-02	1.6E-03	4E-03
5	9E-04	6.5E-05	1.7E-04	3.3E-03	1.4E-04	3.6E-04
10	7.1E-04	1.6E-05	4.2E-05	1.3E-03	6.6E-05	1.7E-04
15	9.7E-04	1.6E-04	4.2E-04	1.2E-03	2.9E-04	7.6E-04
20	8.5E-04	1.3E-04	3.4E-04	7.5E-04	1.5E-04	4E-04
25	9.3E-04	8.1E-05	2.2E-04	2E-03	2.9E-04	7.7E-04

Table 1.
 RMSE, MAE and MAVE at different currents and rotor position.

Comparison of RMSE Error for ANFIS and MVNLRT Inductance Models

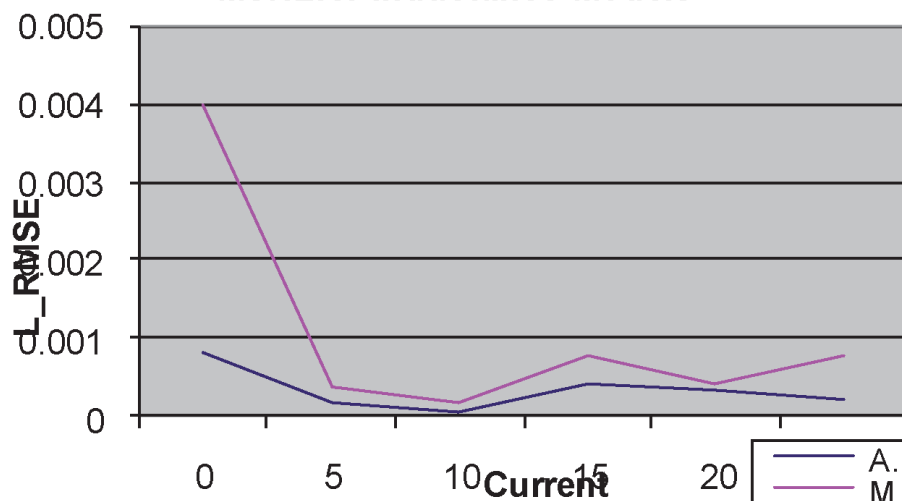


Figure 17.
 L_RMSE - ANFIS vs MVNLRT.

that both ANFIS and MVNLRT models produce accurate mapping between input and output parameters. Among these two methods, ANFIS model has proved to have developed the model with higher precision and with least errors.

6. Conclusion

This paper has presented two methods of computationally efficient modeling techniques for a 3 phase, 6/4 switched reluctance generator for obtaining the nonlinear inductance model by means of adaptive neuro fuzzy inference system and Multivariate nonlinear regression technique. The developed inductance profile based on both these methods is trained with the same set of true data. Both the estimated models depict the nonlinear relation between phase winding inductance at various operating currents and at various rotor positions at each current. MVNLRT predicted model is in good concurrence with the true model. The ANFIS model shows an excellent concurrence with true data and reports only an insignificant error throughout the data range. From the observations and analysis of results

obtained, it is inferred that both the techniques are proficient in estimation of SRM inductance parameter within acceptable accuracy limits. The methods are highly certain in presenting a superior performance when applied to modeling, prediction and control. Both are very simple, easy to implement and are sure to replace any computationally intensive numerical model of SRM. Of the two methods proposed in this chapter, ANFIS has high computational speed, simple structure, least training least epoch, faster learning, good convergence and presents a superior performance. The computational accuracy and easiness of estimation validate that ANFIS is highly competent tool for real time control of SR machine.

IntechOpen

IntechOpen


Author details

Susitra Dhanarajalu

Department of Electrical and Electronics Engineering, Sathyabama Institute of Science and Technology, Chennai, Tamilnadu, India

*Address all correspondence to: susitradhanraj@gmail.com

IntechOpen

© 2021 The Author(s). Licensee IntechOpen. This chapter is distributed under the terms of the Creative Commons Attribution License (<http://creativecommons.org/licenses/by/3.0>), which permits unrestricted use, distribution, and reproduction in any medium, provided the original work is properly cited. 

References

- [1] Osamu Ichinokura, Tsukasa Kikuchi, Kanji Hackamore, Tadakki Watanabe and Hai-Jiao Guo, Dynamic simulation model of switched reluctance generator, *IEEE trans. Magnetics*, Vol. 39, No. 5, pp. 3253–3255, September 2003.
- [2] Loop, B. Essah, D. N. Sudhoff, S., A basis function approach to the nonlinear average value modelling of switched reluctance machines, *IEEE Transaction on energy conversion*, 2006, VOL 21; no 1, pages 60–68.
- [3] Radimov. N, Ben-Hail, N and Rabinovici. R, A Simple Model of Switched-Reluctance Machine Based Only on Aligned and Unaligned Position Data, *IEEE IEEE Transactions on Magnetics*, 2004, vol. 40, issue 3, pp. 1562–1572.
- [4] Loop. B.P, Sudhoff. S.D, Switched reluctance machine model using inverse inductance charecterization, *IEEE Transaction on industry applications*, June 2003, Vol.39, issue.3, pp.743–751.
- [5] Hongwei Gao, Farzad Rajaei salmasi and Ehsani Mehrdad, Inductance model-based sensorless control of the switched reluctance motor drive at low speed, *IEEE transactions on power electronics*, 2004, vol. 19, no 6, pp. 1568–1573.
- [6] Edrington, C.S. Fahimi, and B. Krishnamurthy. M, An autocalibrating inductance model for Switched reluctance motor drives, *IEEE Transaction on Industrial Electronics*, 2007, vol.54, pp.2165–2173.
- [7] Abelardo Martinez, Eduardo Laloya, Javier Vicuna, Francisco perez, Tomas Pollan, Bonifacio Martin, Beatriz Sanchez and Juan Llado, Simulation model of an AC autonomous Switched reluctance generator, EUROCON 2007 - The International Conference on Computer as a Tool (EUROCON 2007), vol.2
- [8] wen ding, deliang Liang, Fourier series and ANFIS based modelling and prediction for switched reluctance motor, International conference on electrical machines and systems, ICEMS 2008.
- [9] Hujjan Zhou, Wen Ding and Zhenmin Yu, A nonlinear model for the Switched reluctance motor, *Proc. of the 8th International conference on Electrical machines and systems*, ICEMS sep 2005, vol.1, pp.568–571.
- [10] Hoang Le-Huy and Patrice Brunelle, A versatile Nonlinear Switched reluctance Motor model in simulink using realistic and analytical magnetization characteristics.
- [11] Vladan Vujcic and Slobodan.N, A simple nonlinear model of the switched reluctance motor, *IEEE Transaction on energy conversion*, Dec 2000, vol.15, No.4.
- [12] Shoujan Song and Weiguo Liu, A novel method for nonlinear modeling and dynamic simulation of a four -phase switched reluctance generator system based on MATLAB SIMULINK, in *Proc. 2007 Second IEEE conference on Industrial Electronics and Applications*, pp. 1509–1514.
- [13] Ustun. O, Measurement and Real-Time Modeling of Inductance and Flux Linkage in Switched Reluctance Motors, *IEEE Transactions on Magnetics*, vol. 45, issue 12, pp. 5376–5382.
- [14] Wenzhe Lu, Ali Keyhani and Abbas Fardoun, Neural network based modelling and parameter identification of switched reluctance motors, *IEEE Transaction on energy conversion*, june 2003, vol.18, no.2
- [15] Zhengyu Lin, Doanld S. Reay, barry. W. Williams and Xiangning He, Online modelling for switched reluctance

motors, *IEEE Transactions on Industrial electronics*, dec 2007, vol.54, no.6.

[16] Xiao Wen-Ping and Ye Jia-wei, Improved PSO-BPNN algorithm for SRG modelling, International Conference on Industrial Mechatronics and Automation, 2009. ICIMA 2009. Volume, Issue, 15–16 May 2009 Page(s): 245–248.

[17] Vejjan. R, Gobbi. R and Sahoo. N.C, Polynomial neural network based modeling of Switched reluctance motors, Power and energy society general meeting-Conversion and delivery of electrical energy in 21st century, July 2008, pp.1–4.

[18] Elmas.C, sagiroglu.S, colak.I and Bal.G, Modeling of non-linear switched reluctance drive based on artificial neural networks, 5th international conference on Power electronics and variable speed drives, Oct 1994, pp.7–12.

[19] Yan cai and Chao Gao, Non-linear modelling of switched reluctance drive based on BP neural networks, *Proc. of the 3rd International Conference on Natural Computation*, 2007, vol.01, pp.232–236.

[20] Oguz Ustun, A nonlinear full model for switched reluctance motor with artificial neural networks, *Energy Conversion and Management*, Sep 2009, vol.50, pp.2413–2421.

[21] Hexu Sun, yanqing Mi, Yan Dang, Yi Zheng and Yanzong Dong, The nonlinear modelling of switched reluctance motor with improved RBF network, second international conference on Intelligent networks and Intelligent systems, 2009.

[22] Wen Ding Deliang Liang, Modeling of a 6/4 Switched Reluctance Motor using adaptive neural fuzzy inference system, *IEEE Transactions on Magnetics*, July 2008, vol.44, issue:7, pp-1796-1804.

[23] Ferhat Daldaban, Nurettin Ustkoyuncu and Kerim Guney, Phase

inductance estimation for switched reluctance motor using adaptive neuro-fuzzy inference system, July 2005, Science Direct.

[24] Susitra, D., Paramasivam S. (2014), “Estimation of phase inductance profile in a three-phase 6/4 pole switched reluctance,” *International Journal of Power Electronics*, vol.6, no.3, pp. 257–274.

[25] Susitra, D. and S. Paramasivam, “Artificial intelligence-based rotor position estimation for a 6/4 pole switched reluctance machine from phase inductance,” *International Journal of modelling, identification and control*, 22(1), pp. 68–79.

[26] R.Krishnan. *Switched reluctance motor drives. Modeling, Simulation, Analysis, Design and Applications* Boca Raton FL: CRC. 2001.

[27] Switched reluctance motor Design and Simulation software by Peter Omand Rasmussen.

[28] J.S.R. Jang, ANFIS: Adaptive-Network-Based Fuzzy Inference System, *IEEE Trans. Systems, Man, Cybernetics*, 23(5/6):665–685, 1993.